Chemical Engineering Journal 159 (2010) 230–235

Contents lists available at ScienceDirect

Chemical Engineering Journal

journal homepage: www.elsevier.com/locate/cej

Radiation synthesis and characterization of protein stabilized gold nanoparticles

A. Akhavan[a], H.R. Kalhor[b,*], M.Z. Kassaee[a], N. Sheikh[c], M. Hassanlou[b]

[a] Chemistry Department, Tarbiat Modares University, Tehran, Iran
[b] Biochemistry Department, Faculties of Biological Sciences, Tarbiat Modares University, Tehran, Iran
[c] Radiation Applications Research School, Nuclear Science and Technology Research Institute, Tehran, Iran

ARTICLE INFO

Article history:
Received 3 November 2009
Received in revised form 3 February 2010
Accepted 5 February 2010

Keywords:
Gold nanoparticles
Radiation
Protein

ABSTRACT

Gold nanoparticles were synthesized in a single step and a facile procedure by γ-irradiation using bovine serum albumin protein as a stabilizer. The results of UV–vis absorption spectroscopy, transmission electron microscopy and X-ray diffraction analyses indicated that spherical well-dispersed gold nanoparticles ranging from 2 to 7 nm were generated, depending on the irradiation doses. The conjugation of BSA to the gold nanoparticles was indicated using FTIR spectroscopy and dynamic light scattering. Moreover, the effect of irradiation on the BSA structure in the presence and absence of Au^{3+} was studied by SDS-PAGE analysis. It became evident that gold nanoparticles formation partially protected against the degradation and aggregation of BSA. Methyl tetrazolium (MTT) assay demonstrated that the generated gold nanoparticles are not cytotoxic to mammalian cells in cultures.

1. Introduction

Gold nanoparticles (Au NPs) have drawn remarkable interest in the past few years because of their potential applications in biomedicines [1,2], biotechnology [3,4], electronics [5], and catalysis [6]. Many stabilizers such as surfactants, polymers, micelles, and ligands have been used to prepare stable colloidal Au NPs or generate a specific property in these particles [7–10]. Recently, stabilization of Au NPs by a variety of biomolecules such as proteins, peptides, DNA, and carbohydrates has been of great interest due to their applications in biomedicine [11–14]. Although several methods have been reported for the preparation of gold colloids in the presence of biopolymers, it is still a challenge to generate these particles with a desired structure, size, and shape in a convenient green way. Hence, the radiation method offers several advantages for the preparation of colloidal metal nanoparticles [15–18]. In this method hydrated electrons produced during the water radiolysis can reduce metal ions at the ambient temperature without using excessive reducing agents and consequent side reactions. Moreover, the electrons can be uniformly distributed in the solution, and therefore metal nanoparticles are produced in uniformly dispersed, fully reduced, highly pure, and highly stable forms. More importantly, the size of nanoparticles can be controlled by varying the dose of irradiation [19]. Although γ-irradiation method was employed to synthesize gold nanoparticles in the presence of various stabilizers [16–18], to our knowledge there has not been a report on the synthesis of Au NPs in the presence of a protein using radiation.

Bovine serum albumin (BSA) is a model globular protein which is widely used in biochemical studies [20,21]. It is composed of 583 amino acid residues containing several sulfur, oxygen and nitrogen atoms, which are generally used to stabilize the nanoparticles [22]. In this study, we have synthesized BSA stabilized Au NPs via γ-irradiation method. The generated Au NPs at various irradiation doses were characterized by TEM, XRD, FTIR, and DLS. Methyl tetrazolium (MTT) assay was also used to examine the particles cytotoxicity. SDS-PAGE technique was used to study the BSA structure. Because the generation of Au NPs takes place in presence of a biopolymer in aqueous medium without using a reducing agent, our method can be considered as a green approach for generating Au NPs which can be of importance for pharmaceutical and biomedical applications.

2. Materials and methods

2.1. Materials

Bovine serum albumin (BSA) and $HAuCl_4$ were purchased from Merck. The BSA solutions were prepared in 0.01 M phosphate buffer solution (PBS) of pH 7.4. All reagents were used as received without further purification. Double distilled water was used throughout the experiments.

* Corresponding author. Tel.: +98 2182883419.
E-mail address: hrkalhor@modares.ac.ir (H.R. Kalhor).

1385-8947/$ – see front matter © 2010 Elsevier B.V. All rights reserved.
doi:10.1016/j.cej.2010.02.010

2.2. Gold nanoparticles synthesis

In a typical experiment, four 20 ml sample solutions containing $HAuCl_4$ (5×10^{-4} M), and BSA (6×10^{-6} M) were prepared in the PBS buffer. The mixtures were stirred using a magnetic stirrer at room temperature for 20 min. Similarly, samples without BSA were also prepared for comparison. Then, all samples were purged with nitrogen and irradiated to 2.5, 5, and 10 kGy (7, 15, and 30 min irradiation time, respectively) doses at room temperature. Irradiation was performed in a Gammacell-220 (Nordion, Canada), ^{60}Co source with 5.4 Gy/s dose rate, calibrated by Fricke dosimeters. After irradiation, the mixtures were stirred at room temperature for 20 min and then stored at 4 °C prior to use for characterization. For isolation of nanoparticles, the BSA stabilized gold nanoparticles were centrifuged at 17,000 rpm for 1 h at 10 °C. The collected nanoparticles were resuspended in PBS solution and centrifuged as above for three times to insure the complete removal of free BSA.

2.3. Characterization techniques

UV–vis spectra were recorded at room temperature on a Unicame spectrophotometer in the wavelength region 200–600 nm. TEM were performed using ZEISS-EM 900 microscope operating at 80 kV. Samples for TEM characterization were prepared by depositing a drop of Au NPs solution on a coated copper grid and then drying at room temperature. DLS measurements were performed at room temperature using a Malvern Zetasizer having red laser at a wavelength of 633 nm. FTIR spectra of the samples were obtained using a Nicolet (Nexus 870) FTIR spectrophotometer. All spectra of the samples were taken via the ATR method with a resolution of 4 cm^{-1}. Second-derivative spectra were obtained with the derivative function of Omnic software [23]. SDS-PAGE was performed according to the method of Laemmli [24]. Identical concentrations of BSA solutions (6×10^{-6} M) were loaded on each lane for comparison, separated with 4% stacking and 12% resolving gel, and stained with Coomassie Blue.

2.4. In vitro cytotoxicity test

Human cancer cell lines regularly grown in Dulbecco's modified Eagle's medium (DMEM) with 10% fetal calf serum (FCS) 100 units/mL penicillin, and 100 mg/mL streptomycin in a humidified atmosphere of 5% CO_2 and 95% air at 37 °C. Cells in their exponential phase of growth were seeded at a density of 5×10^3 cells/well of a 96-well tissue culture plate and incubated for 24 h. The cells were treated for 4 h with different concentrations of purified gold nanoparticles that were generated at 5 kGy. Control cells were used without nanoparticle treatment. At the end of each exposure, the toxicity level of nanoparticles was assessed by 3-(4,5-dimethylazol-2-yl)-2,5-diphenyl-tetrazolium bromide (MTT) assay. The MTT assay helps in cell-viability assessment by measuring the enzymatic reduction of yellow tetrazolium MTT to a purple formazan [25]. The measurement was performed by ELISA reader (Multiscan MS; Labsystem). All experiments were carried out in quadruplets, and the average of all of the experiments has been shown as cell-viability percentage in comparison with the control experiment, while gold untreated controls were considered as 100% viable.

3. Results and discussions

We have synthesized BSA stabilized Au NPs via γ-irradiation of aqueous solution containing Au^{3+} ions in a single step. In this method hydrated electrons, produced during the irradiation, reduce the metal ions to zero-valent atoms, which coalesce to grow into larger clusters and eventually into the precipitates [16,17]. The metal cluster coalescence should be limited by a molecule as a cluster stabilizer to find metal particles in nano-scale size. Here the produced gold clusters in the early stages are stabilized by BSA, through the electrostatic repulsion, steric hindrance or the presence of functional groups such as thiols and carboxylates, leading to the formation of Au NPs.

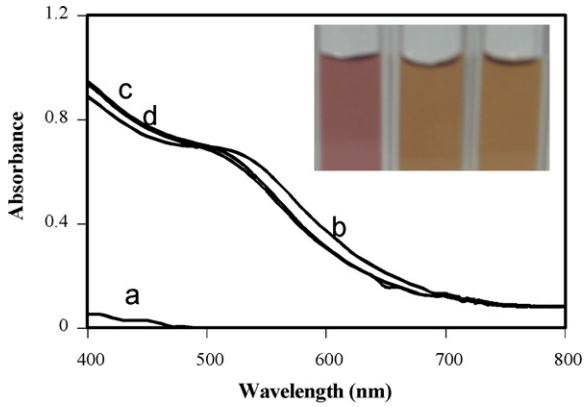

Fig. 1. The UV–vis spectra of the BSA stabilized Au NPs at: (a) 0, (b) 2.5, (c) 5 and (d) 10 kGy irradiation doses. The gold concentration used in the starting material was 5×10^{-4} M. The inset shows the BSA stabilized Au NPs solutions in 2.5, 5, and 10 kGy (left to right, respectively).

We used UV–vis spectroscopy to examine the generation of Au NPs in the presence of BSA using γ-irradiation. At first, the reduction of Au^{3+} solutions, without the addition of BSA, was investigated at γ-ray doses ranging from 2.5 to 10 kGy by recording the UV–vis spectrum of the sample solutions (data not shown). As the irradiation dose increased from 2.5 to 10 kGy, the Au^{3+} ions reduced to Au atoms and precipitated as a solid metal. However, when the Au^{3+} solutions were irradiated in the presence of BSA a different trend was observed. The UV–vis absorption spectra of Au NPs prepared in various doses in the presence of BSA is indicated in Fig. 1. After the irradiation, at 2.5 kGy the solution turn purple whereas both solutions exposed at 5 and 10 kGy turn pale brown (Fig. 1, inset). The Au NPs absorption band, which is generally located around 520 nm, is detected for the three exposed solutions. Upon increasing the irradiation dose, from 2.5 to 5 kGy, the plasmon band become flatter and shifts to a slightly shorter wavelength, indicating the formation of smaller particles at 5 kGy [17]. The spectra of the irradiated solutions at 5 and 10 kGy are quite similar suggesting that the total reduction of Au^{3+} occurs at 5 kGy and the size and shape of the generated Au NPs in both solutions are most likely the same. All in all, the results indicate that when irradiation dosage increases, more nucleation would be followed by successive growth of the particles. Increasing the number of nucleus may cause the smaller particles at higher dosages to be formed as it has been suggested previously [18]. We also found that the size distribution of the Au NPs depends on the concentration of BSA. The UV–vis spectra of the sample irradiated at 5 kGy is shown in Fig. 2. When the BSA concentration increases from 0.4×10^{-6} to 3×10^{-6} M, the corresponding plasmon band at 530 nm shows a blue shift from 530 to 525 nm, indicating the formation of smaller particles [17,18]. Upon increasing the BSA concentration from 3×10^{-6} to 6×10^{-6} M, the absorption spectrum becomes flatter, suggesting the formation of smaller Au NPs at higher concentration of BSA. Altogether, the results from Fig. 2 show that when the BSA concentration is increased, the stabilization occurs more effectively, giving rise to smaller nanoparticles.

To evaluate the stability of the Au NPs, absorption spectra of the samples were obtained after 4 months. No remarkable changes

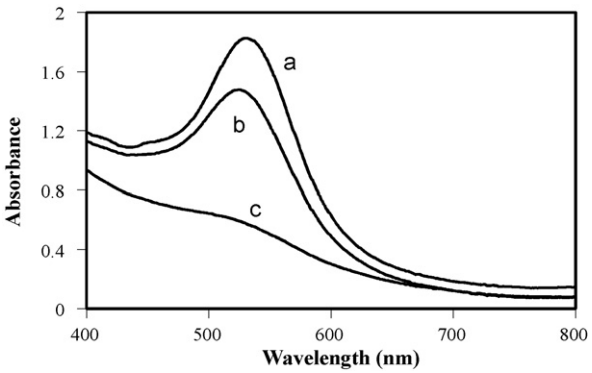

Fig. 2. The UV–vis spectra of the BSA stabilized Au NPs generated at 5 kGy at different concentration of BSA: (a) 0.4×10^{-6} M, (b) 3×10^{-6} M, and (c) 6×10^{-6} M.

were observed in the spectra, suggesting that the BSA stabilized Au NPs prepared under gamma irradiation are stable over a long period which could be important for their applications.

TEM was performed to observe directly the Au NPs generated at 2.5, 5, and 10 kGy. As shown, in Fig. 3(A–C), the Au NPs made in all irradiation doses are in the spherical shape and well-separated form without any notable aggregation. Using X-ray diffraction, these particles turned out to have a face centered cubic (fcc) crystal structure (data not shown). Additionally, the TEM micrographs and their corresponding size distribution histograms demonstrate that the mean size of the nanoparticles at 2.5, 5, and 10 kGy are about 7.5, 2.7, and 2.3 nm, respectively (Fig. 3). The TEM data confirm that the size of particles at the dose of 2.5 kGy is larger than that in the 5 and 10 kGy. Not a great change is observed in the mean size of generated nanoparticles at 5 and 10 kGy, in agreement with their UV–vis results (Fig. 1).

In order to examine the particles size distribution, DLS was also performed and its results were compared to the TEM data. The particle size obtained from DLS measurements for all absorbed doses is obviously larger than the TEM results because DLS analysis measures the hydrodynamic radius which takes into consideration the BSA layer on the surface of the gold as well. At the dose of 2.5 kGy, the DLS size distribution indicates the nanoparticles with mean size of about 14 nm in diameter. When the irradiation dose is increased from 2.5 to 5 kGy, in addition to the nanoparticles of 12 nm, another distribution peak appears at 25 nm; subsequently, the larger peak at 28 nm become the sole peak at the dose of 10 kGy (Fig. 4). Considering the size of BSA (8.4 nm) [26] and our TEM results, the increasing nanoparticles size and the large size distribution in DLS data could be attributed to the conjugation of BSA to Au NPs. The enlarging of the BSA layer at higher γ-irradiation doses most likely can be explained by the presence of reactions such as cross-linking reactions as has been previously

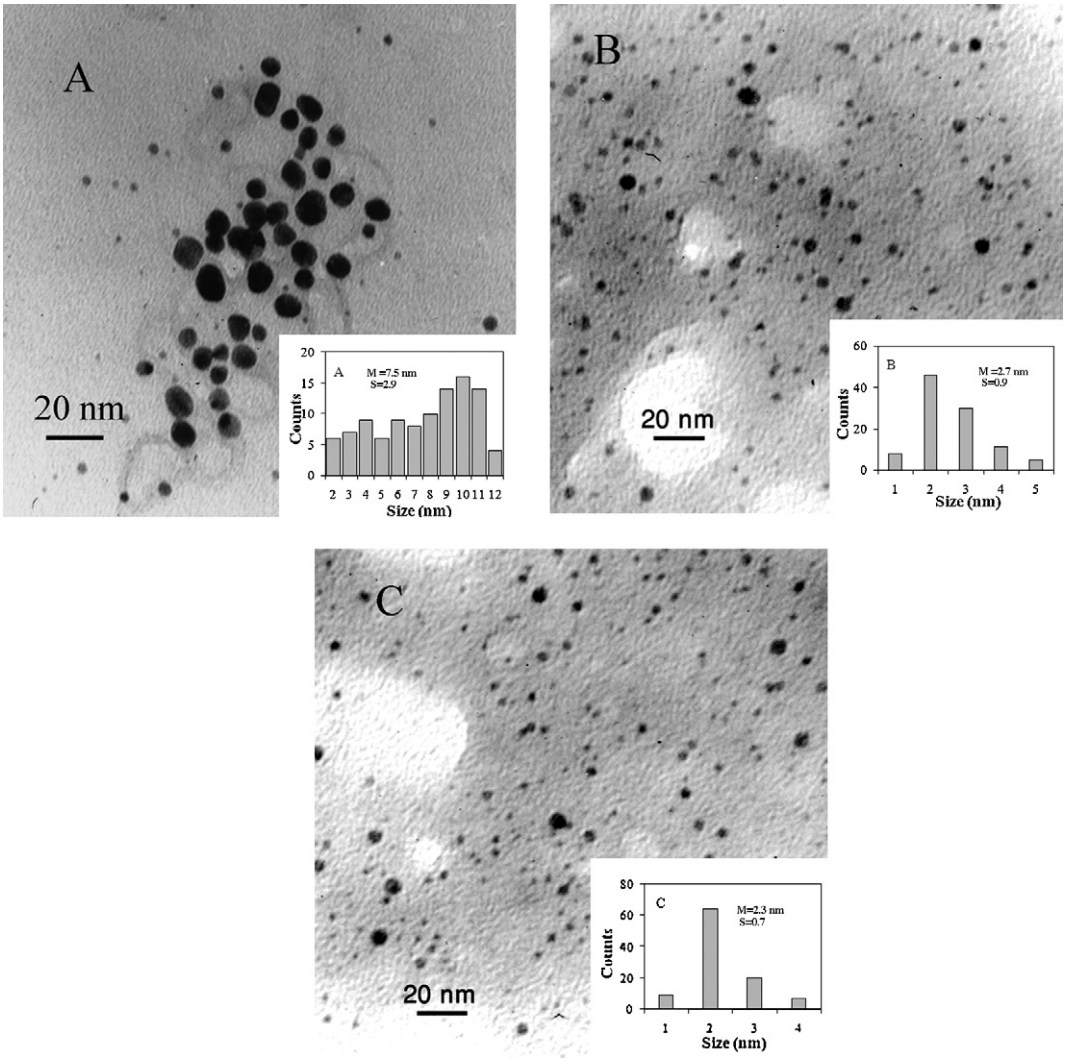

Fig. 3. TEM image and the corresponding size distribution of BSA stabilized Au NPs at various doses: (A) 2.5, (B) 5, and (C) 10 kGy.

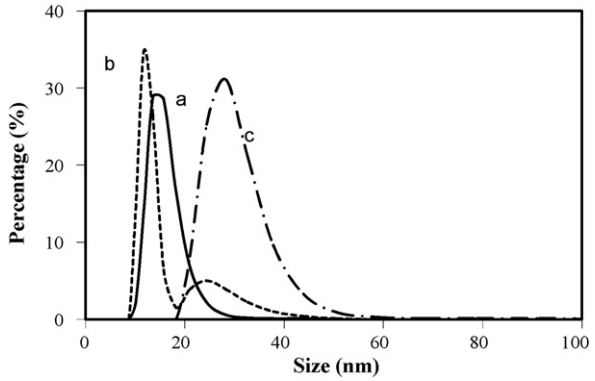

Fig. 4. DLS analysis of BSA stabilized Au NPs prepared at the dose of (a) 2.5, (b) 5, and (c) 10 kGy.

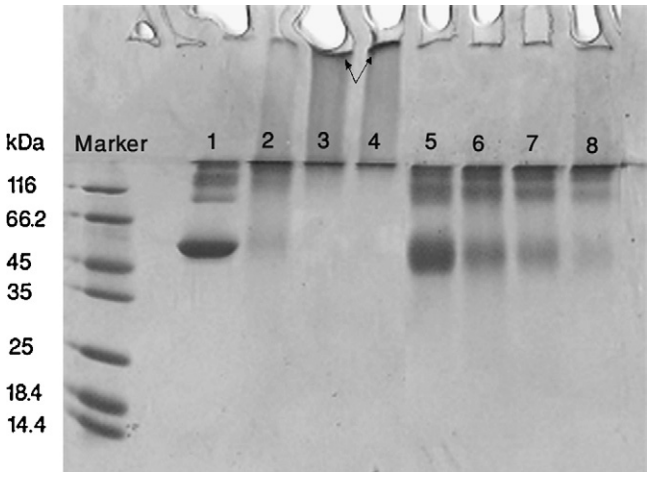

Fig. 6. SDS-PAGE profile of: BSA without Au^{3+} (1–4) irradiated at the dose of 0, 2.5, 5, and 10 kGy, respectively, and BSA containing Au^{3+} (5–8) irradiated at 0, 2.5, 5, and 10 kGy, respectively. The arrow labels the aggregation of proteins that did not enter the gel.

suggested to occur during the exposure of proteins to irradiation [27–29].

To further study the structural changes that the BSA molecules undergo on the nanoparticles surface, FTIR spectroscopy was used as a valuable technique (Fig. 5). The native BSA shows the amide I band of the peptide group in the 1615, 1629, and 1640 cm^{-1} (β-sheet), 1658 cm^{-1} (α-helix), and 1667, 1674, and 1685 cm^{-1} (turn) positions. The positions of these peaks do not undergo any remarkable change in the BSA stabilized Au NPs. However, comparing to native BSA, obvious differences are observed in the shape of the peaks for both the irradiated BSA and BSA stabilized Au NPs, suggesting the occurrence of changes in the secondary structure of the albumin during irradiation. More detailed information about these conformational changes is obtained by analyzing the second-derivative spectrum of original FTIR spectrum (Fig. 5B) [23]. As shown, the intensity band for α-helix (1658 cm^{-1}) is decreased in irradiated BSA and BSA stabilized Au NPs (Fig. 5B panel b, c) in comparison to native BSA.

Generally, the radiation-induced chemical changes in protein molecules are caused by products of water radiolysis through the formation of hydrated electrons and hydroxyl radicals [28]. In this method, these reactive species are mainly involved in the generation of Au NPs. With this in mind, we found it worthwhile to study the effect of irradiation on the BSA structure in presence and absence of Au^{3+} by SDS-PAGE analysis (Fig. 6). SDS-PAGE profiles of the irradiated BSA at 2.5 kGy shows a slight breakdown of the polypeptide chain along with the negligible aggregated molecules. Above 2.5 kGy at the dose of 5 and 10 kGy, there is a significant increase in the aggregated proteins which could not penetrate into the gel (arrows). These higher molecular weight aggregates can be attributed to the cross-linked products of the degraded protein

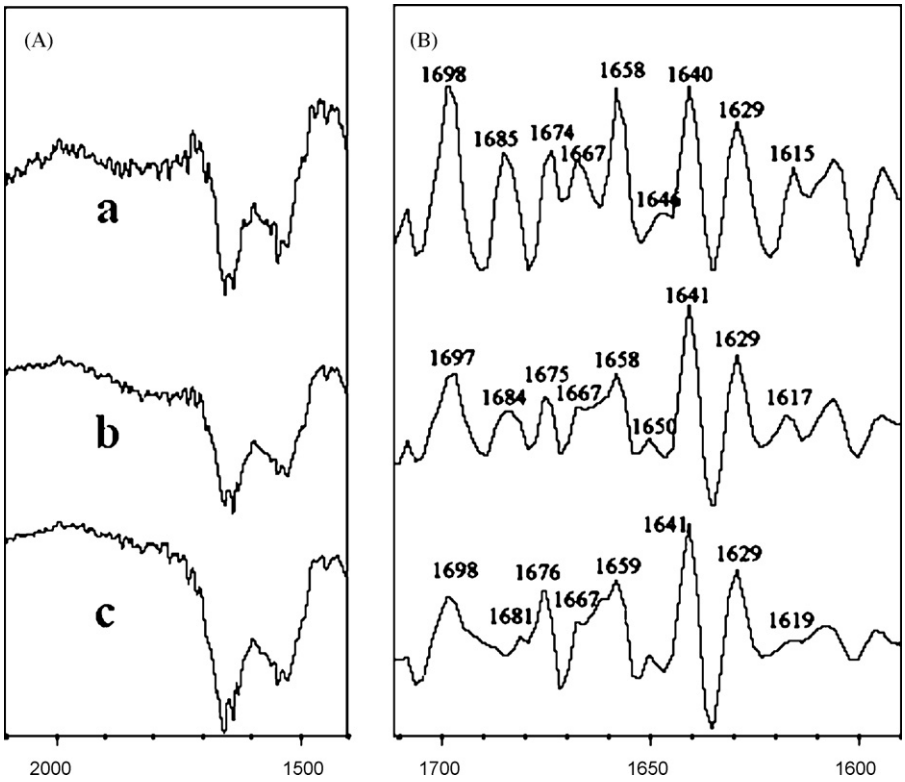

Fig. 5. FTIR spectra of the (a) BSA, (b) irradiated BSA, (c) BSA stabilized Au NPs generated at 5 kGy (A) and corresponding second-derivative spectra (B) in the amide I region.

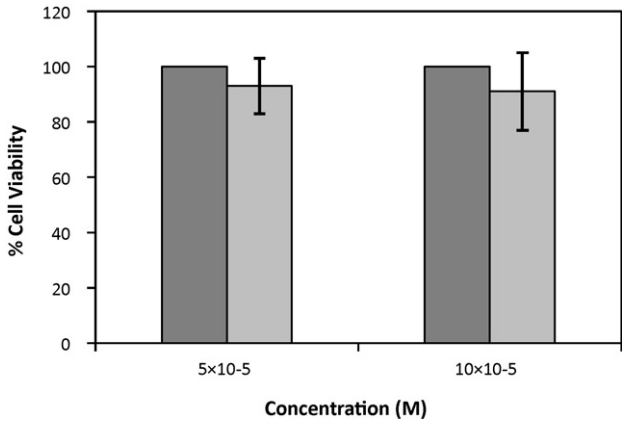

Fig. 7. Cytotoxicity assessment (MTT assay) of BSA stabilized Au NPs at various concentrations tested against Hela cell lines. The concentration of nanoparticles was best estimated by the method used in [30]. Dark columns: controls (untreated cells), light columns: BSA stabilized Au NPs.

[26,27]. Interestingly, when the BSA is exposed to 2.5, 5, and 10 kGy in the presence of Au^{3+}, the major band of the BSA are somewhat maintained (compared to the absence of Au^{3+}) and the aggregated protein decreases for all absorbed doses especially for 5 and 10 kGy. The SDS-PAGE analysis illustrates that the formation of Au NPs partially protects against the aggregation of irradiated protein. Most likely, in the presence of Au^{3+} considerable parts of the generated initial radicals such as e_{aq}^- are consumed by the reduction of Au^{3+} leading to the formation of Au NPs; thus, these species are less involved in protein breakdown or cross-linking reactions. Therefore, from our data it can be deduced that the concentration of Au^{3+} may influence the amount of protein protection during nanoparticles formation; this effect could be further examined using different concentration of gold. In addition, formation of nanoparticles using other metals such as silver can also have different effects from the gold in protecting the proteins. The comparison of different type of metal nanoparticles can better illuminate the mechanisms of protein protection when exposed to γ-ray.

Since BSA conjugated nanoparticles are potentially utilized for pharmaceutical and biomedical applications one must assay their cytotoxicity. To check the cytotoxicity of BSA stabilized Au NPs, MTT assay was performed. The viability results show that at both concentrations of 5×10^{-5} and 10×10^{-5} M of BSA stabilized Au NPs more than 90% cell viability is seen for Hela cells, indicating the particles cytocompatibility (Fig. 7). However, it must be mentioned that in much higher concentration of the nanoparticles, the nanopaticles might become cytotoxic to the cells.

4. Conclusion

In this work, we demonstrated that in a single step procedure, γ-irradiation can be used to generate well-disperse spherical nanoparticles when BSA is used as a stabilizer. The nanoparticle size and distribution are influenced by the amount of irradiation and the protein concentration. The conjugation of BSA to Au NPs is confirmed by FTIR and DLS techniques. However, the secondary structure of BSA conjugated to Au NPs is not maintained and is changed from the native protein structure. Further, the SDS-PAGE analysis illustrated that the formation of Au NPs can partially protect against the aggregation of irradiated protein. The generated nanoparticles show no cytotoxicity to the mammalian cells in cultures. Our method for producing cytocompatible Au NPs can also be considered as a green method since it takes place in aqueous medium in the presence of a biopolymer, without usage of any reducing agent. The green approach to synthesis of gold nanoparticles is crucial for their pharmaceutical and biomedical applications.

Acknowledgements

This work was supported in part by Tarbiat Modares University. The authors would like to thank Mr. M. Kamizi for technical assistance.

References

[1] X. Zhou, X. Zhang, X. Yu, X. Zha, Q. Fu, B. Liu, X. Wang, Y. Chen, Y. Chen, Y. Shan, Y. Jin, Y. Wu, J. Liu, W. Kong, J. Shen, The effect of conjugation to gold nanoparticles on the ability of low molecular weight chitosan to transfer DNA vaccine, Biomaterials 29 (2008) 111–117.
[2] T. Liu, J. Tang, L. Jiang, The enhancement effect of gold nanoparticles as a surface modifier on DNA sensor sensitivity, Biochem. Biophys. Res. Commun. 313 (1) (2004) 3–7.
[3] C.D. Medley, J.E. Smith, Z. Tang, Y. Wu, S. Bamrungsap, W. Tan, Gold nanoparticle-based colorimetric assay for the direct detection of cancerous cells, Anal. Chem. 80 (2008) 1067–1072.
[4] M. Scampicchio, A. Arecchi, S. Mannino, Optical nanoprobes based on gold nanoparticles for sugar determination, Nanotechnology 20 (13) (2009) 135501–135505.
[5] A. Labande, J. Ruiz, D. Astruc, Supramolecular gold nanoparticles for the redox recognition of oxoanions: syntheses, titrations, stereoelectronic effects, and selectivity, J. Am. Chem. Soc. 124 (2002) 1782–1789.
[6] Z. Liu, P. Hu, Catalytic role of gold in gold-based catalysts: a density functional theory study on the CO oxidation on gold, J. Am. Chem. Soc. 124 (2002) 14770–14779.
[7] M. Brust, M. Walker, D. Bethell, D.J. Schiffrin, R.J. Whyman, Synthesis of thiol-derivatized gold nanoparticles in a two phase liquid–liquid system, J. Chem. Soc., Chem. Commun. (1994) 801–802.
[8] M.K. Corbierre, N.S. Cameron, R.B. Lennox, Polymer-stabilized gold nanoparticles with high grafting densities, Langmuir 20 (2004) 2867–2873.
[9] S.R. Johnsona, S.D. Evans, S.W. Mahonb, A. Ulmanc, Synthesis and characterisation of surfactant-stabilised gold nanoparticles, Supramol. Sci. 4 (1997) 329–333.
[10] M.G. Spirin, S.B. Brichkin, V.F. Razumov, Synthesis and stabilization of gold nanoparticles in reverse micelles of aerosol OT and Triton X-100, Colloid J. 67 (4) (2005) 485–490.
[11] S.T. Hussain, M. Iqbal, M. Mazhar, Size control synthesis of starch capped–gold nanoparticles, J. Nanoparticle Res. 11 (6) (2009) 1383–1391.
[12] A.J. Ryan, W.K. Overton, E.M. Speight, N.C. Oldenburg, L. Loo, W. Robarge, S. Franzen, L.D. Feldheim, Cellular uptake of gold nanoparticles passivated with BSA-SV40 large T antigen conjugates, Anal. Chem. 79 (2007) 9150–9159.
[13] L. Shang, Y. Wang, J. Jiang, S. Dong, pH-Dependent protein conformational changes in albumin-gold nanoparticle bioconjugates: a spectroscopic study, Langmuir 23 (2007) 2714–2721.
[14] M.J. Bergen, A.H. Recum, T.T. Goodman, P.A. Massey, H.S. Pun, Gold nanoparticles as a versatile platform for optimizing physicochemical parameters for targeted drug delivery, Macromol. Biosci. 6 (2006) 506–516.
[15] J. Belloni, M. Mostafavi, H. Remita, J.L. Marignier, M.O. Delcourt, Radiation-induced synthesis of mono- and multimetallic clusters and nanocolloids, New. J. Chem. 22 (1998) 1239–1255.
[16] E. Gachard, H. Remita, J. Khatouri, B. Keita, L. Nadjo, J. Belloni, Radiation-induced and chemical formation of gold clusters, New J. Chem. 22 (1998) 1257–1265.
[17] A. Henglein, Radiolytic preparation of ultrafine colloidal gold particles in aqueous solution: optical spectrum, controlled growth, and some chemical reactions, Langmuir 15 (1999) 6738–6744.
[18] T. Liu, H.G. Park, S.-H. Choi, γ-Irradiation-induced preparation of Ag and Au nanoparticles and their characterizations, Mater. Chem. Phys. 105 (2007) 325–330.
[19] A. Henglein, D. Meisel, Radiolytic control of the size of colloidal gold nanoparticles, Langmuir 14 (1998) 7392–7396.
[20] J.M. Meziani, P. Pathak, A.B. Harruff, R. Hurezeanu, Y.-P. Sun, Direct conjugation of semiconductor nanoparticles with proteins, Langmuir 21 (2005) 2008–2011.
[21] K.U. Hansen, Molecular aspects of ligand binding to serum albumin, Pharmacol. Rev. 33 (1981) 17–53.
[22] S.H. Brewer, W.R. Glomm, M.C. Johnson, M.K. Knag, S. Franzen, Probing BSA binding to citrate-coated gold nanoparticles and surfaces, Langmuir 21 (2007) 9303–9307.
[23] A. Dong, P. Huang, W.S. Caughy, Protein secondary structure in water from second-derivative amide I infrared spectra, Biochemistry 29 (1990) 3303–3308.
[24] U.K. Laemmli, Cleavage of structure of proteins during the assembly of the head of bacteriophage T4, Nature 227 (1970) 680–685.
[25] T. Mosmann, Rapid colorimetric assay for cellular growth and survival: application to proliferation and cytotoxicity assays, J. Immunol. Methods 65 (1983) 55–63.
[26] M.L. Ferrer, R. Duchowicz, B. Carrasco, J.G. de la Torre, A.U. Acuna, The conformation of serum albumin in solution: a combined phosphores-

cence depolarization-hydrodynamic modeling study, Biophys. J. 80 (2001) 2422–2430.
[27] W.M. Garrison, Reaction mechanisms in the radiolysis of peptides, polypeptides, and proteins, Chem. Rev. 87 (1987) 381–398.
[28] M.H. Gaber, Effect of gamma-irradiation on the molecular properties of bovine serum albumin, J. Biosci. Bioeg. 100 (2) (2005) 203–206.
[29] M. Le Maire, L. Thauvette, B. De Foresta, A. Viel, G. Beauregard, M. Potier, Effects of ionizing radiations on proteins, Biochem. J. 267 (1990) 431–439.
[30] X. Liu, M. Atwater, G. Wang, Q. Huo, Extinction coefficient of gold nanoparticles with different sizes and different capping ligands, Colloids Surf. B: Biointerfaces 58 (2007) 3–7.